Neuroscience 177 (2011) 195–206

RESTORATIVE EFFECT OF INTRACEREBROVENTRICULAR INSULIN-LIKE GROWTH FACTOR-I GENE THERAPY ON MOTOR PERFORMANCE IN AGING RATS

F. NISHIDA,[a1] G. R. MOREL,[b1] C. B. HEREÑÚ,[b] J. I. SCHWERDT,[b] R. G. GOYA[b] AND E. L. PORTIANSKY[a]*

[a]*Institute of Pathology, School of Veterinary Sciences, National University of La Plata, La Plata 1900, Argentina*

[b]*INIBIOLP-Histology B, School of Medicine, National University of La Plata, La Plata 1900, Argentina*

Abstract—Insulin-like growth factor-I (IGF-I) is a powerful neuroprotective molecule in the brain and spinal cord. We have previously shown that intracerebroventricular (i.c.v.) IGF-I gene therapy is an effective strategy to increase IGF-I levels in the cerebrospinal fluid (CSF). Since aging in rats is associated with severe motor function deterioration, we implemented i.c.v. IGF-I gene therapy in very old rats (30–31 months) and assessed the beneficial impact on motor performance. We used recombinant adenovectors (RAds) expressing either green fluorescent protein (GFP) or rat IGF-I. Injection in the lateral or fourth ventricle led to high transgene expression in the ependymal cell layer in the brain and cervical spinal cord. RAd-IGF-I-injected rats but not RAd-GFP-injected controls, showed significantly increased levels of CSF IGF-I. Motor tests showed the expected age-related decline in aged rats. Seventeen-day IGF-I gene therapy induced a significant improvement in motor performance in the aged but not in the young animals. These results show that IGF-I is an effective restorative molecule in the aging brain and spinal cord. The data also reveal that the ependymal route constitutes a promising approach for implementing protective IGF-I gene therapy in the aging CNS.

Key words: cerebral ventricles, spinal cord, IGF-I, ependyma, Qdots.

Insulin-like growth factor-I (IGF-I) is a powerful neurotrophic molecule which by itself or associated to other neuroprotective factors, appears to be part of the physiologic self-repair mechanisms of the adult brain (Sonntag et al., 2005; Carro et al., 2006; García-Segura et al., 2007) and spinal cord (Bilak et al., 2001). Furthermore, there is clear evidence that IGF-I plays a physiologic role in neuroprotection. Thus, IGF-I is strongly induced in the CNS after different insults such as ischemia (Beilharz et al., 1998), cortical injury (Walter et al., 1997; Li et al., 1998) and spinal cord lesions (Yao et al., 1995). Moreover, intraparenchymal IGF-I administration targeted to spinal cord motor neurons of aging mice prevented the typical age-related alterations to the nerve terminals at the neuromuscular junctions (Payne et al., 2007).

Although some IGF-I is produced in the CNS, most of the peptide used by the brain comes from the circulation (Carro et al., 2000, 2006). Serum IGF-I is actively transported through the choroid plexus and translocated to the cerebrospinal fluid (CSF) from where the molecule reaches specific areas of the brain and possibly the spinal cord, by yet unidentified mechanisms (Guan et al., 1996; Carro et al., 2006).

A number of functional and morphologic changes in the spinal cord of aging rats have been documented. Thus, Burek (1978) described a process of demyelination, distended axon sheaths, swollen or absent axons and numerous swollen astrocytes in WAGxBN 30 month old male, but not female rats showing a high prevalence of paralysis or severe paresis of the hind limbs and atrophy of the skeletal muscles in the lumbar region and hind limbs. Nevertheless, no increase in the expression of GFAP (Kane et al., 1997) or S-100 (Fontana et al., 2009) marker was detected in aged rats, which suggests that normal spinal cord aging is not associated to inflammatory processes. In the spinal cord of aging female rats we described variations in size of the organ as well as differences in white and gray matter but not gross morphologic alterations (Fontana et al., 2009). We also reported a complete loss of neuron-specific nuclear protein (NeuN) immunoreactivity in cervical, thoracic and lumbar segments of aged female rats whereas neuron specific enolase immunoreactivity was comparable in young and aged animals (Portiansky et al., 2006). A decrease in the expression of PTEN, a tumor suppressor gene known to play an important role in the regulation of cell size has been also reported in the spinal cord of aging rats (Rodrigues de Amorim et al., 2010). At functional level a marked decline in motor coordination and grip strength does occur in aged female rats (Sanchez et al., 2008).

Profiting from the fact that adenoviral vectors have high affinity for the ependymal cell layer (Hereñú et al., 2009) we used the ependymal route to implement IGF-I gene therapy in aging rats, a treatment that significantly restored motor performance in these animals. Using fluorescent nanoparticles we also demonstrated a physical continuity of the central canal of the fourth ventricle with the central canal of the spinal cord.

[1] These two authors contributed equally to this work.

*Corresponding author. Tel: +54-221-423-6663 x 426; fax: +54-221-425-7980.
E-mail address: elporti@fcv.unlp.edu.ar (E. L. Portiansky).

Abbreviations: ALS, amyotrophic lateral sclerosis; CSF, cerebrospinal fluid; DAPI, 4',6-diamidino-2-phenylindole; GFP, green fluorescent protein; i.c.v., intracerebroventricular; IGF-I, insulin-like growth factor-I; LV, lateral ventricles; Qdots, quantum dots; RAd, recombinant adenoviral vector; 4V, fourth ventricle.

0306-4522/11 $ - see front matter
doi:10.1016/j.neuroscience.2011.01.013

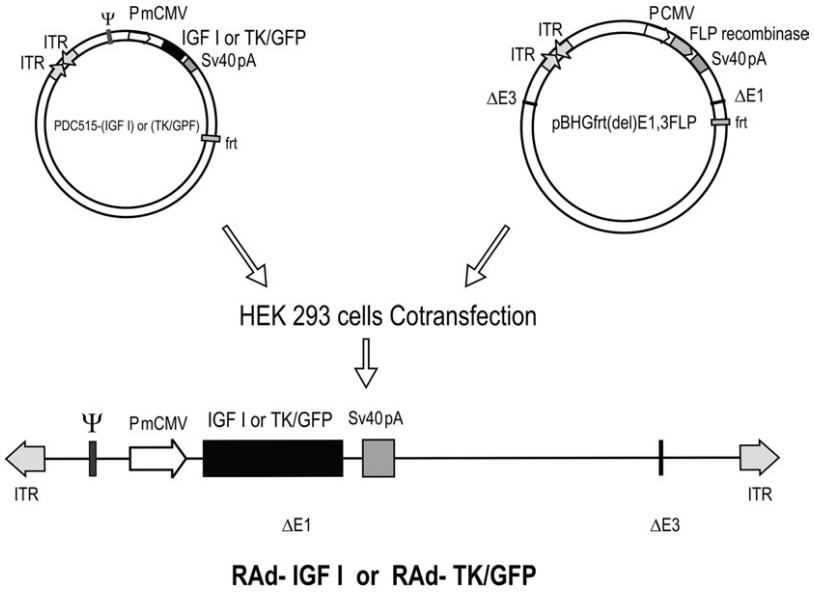

Fig. 1. Diagrammatic representation of the construction of RAd-IGF-I and RAd(TK/GFP)$_{fus}$. The vectors were constructed by the two-plasmid method as described in Experimental procedures. PmCMV, mouse cytomegalovirus promoter; IGF-I, cDNA for rIGF-I; TK/GFP, hybrid DNA sequence encoding the fusion protein (TK/GFP)$_{fus}$; ITR, inverted terminal repeat; ΔE1 and ΔE3, deletions in the Ad5 genome; SV40, simian virus 40 polyadenylation signal; Ψ, packaging signal; frt, recombination site for the FLP recombinase.

EXPERIMENTAL PROCEDURES

Adenoviral vectors

RAd-IGF-I. A RAd vector harboring the rat IGF-I gene (kindly donated by Dr. Peter Rotwein, Oregon Health Sciences University) was constructed in our laboratory by a variant of the two plasmid method (Hitt et al., 1998) as previously described (Hereñú et al., 2007). The cDNA coding for the rat IGF-I gene obtained from the mRNA for the IGF-Ib precursor form (Daughaday and Rotwein, 1989), was placed under the control of the mouse cytomegalovirus (mCMV) promoter in order to construct the genome of the desired recombinant adenoviral vector, RAd-IGF-I (Fig. 1). The newly generated RAd was rescued from HEK293 cell lysates and plaque purified. It was further purified by ultracentrifugation in a CsCl gradient. Final virus stock was titrated by a serial dilution plaque assay.

RAd-(TK/GFP)$_{fus}$. This vector was constructed following the general procedures outlined above (Fig. 1). The vector harbors a hybrid gene encoding the herpes simplex virus type 1 (HSV-1) thymidine kinase fused to the *Aequorea victoria* enhanced green fluorescent protein (TK/GFP)$_{fus}$ (a kind gift from Dr. Jacques Galipeau, McGill University, Montreal, Canada). The corresponding gene product, fusion protein (TK/GFP)$_{fus}$, is targeted to the nucleus where it emits green fluorescence with high intensity when it is excited with 470-nm wideband light (Paquin et al., 2001). This hybrid gene is also driven by the mCMV promoter. The vector was expanded in 293 cells and purified and titrated as indicated above.

Quantum dots

Quantum dots (Qdots) 655^{TM} (Quantum Dot Corporation, Hayward CA, USA) which are elongated nanocrystals (average nanoparticle dimensions 15×8 nm) that strongly fluoresce in the far red (655 nm) were diluted in PBS to achieve a 20 nM final concentration of and intracerebroventricularly (i.c.v.) administered to the animals as described below.

Animals and surgical procedures

Animals. Fifteen young (3–4 months) and 12 aged (30–31 months) female Sprague–Dawley rats were used. Animals were housed in a temperature-controlled room (22±2 °C) on a 12:12 h light/dark cycle. Food and water were available *ad libitum*. All experiments with animals were performed according to the Animal Welfare Guidelines of NIH (INIBIOLP's Animal Welfare Assurance No A5647-01).

Stereotaxic injections. On Experimental day 0 rats were anesthetized with ketamine hydrochloride (40 mg/kg; i.p.) plus xylazine (8 mg/kg; i.m.) and placed in a stereotaxic apparatus. In order to access the lateral ventricles (LV), the tip of a 26G needle fitted to a 50 μl syringe was brought to the following coordinates relative to the bregma: −0.8 mm anteroposterior, 3.7 mm dorsoventral and ±1.5 mm mediolateral (Paxinos and Watson, 1998). On day 0 rats were injected bilaterally with 10 μl per side of a suspension containing 10^{11} plaque forming units (pfu)/ml of the appropriate vector. On experimental day +16, blood was sampled (0.3–0.4 ml) by puncture of the tail veins whereas CSF samples were taken as described below. Serum and CSF samples were stored at −70 °C.

In three animals, 20 μl of the reporter vector was injected at the following coordinates relative to the bregma: −13.3 mm posterior, 7.5 mm dorsoventral, and 0 mm mediolateral (at the midline), in order to access the fourth ventricle (4V) region, caudal to the lateral recesses. Three young rats were injected in the same coordinates of the 4V with 10 μl PBS containing 20 nM Qdots (see above—Quantum dots).

CSF collection

On Experimental day +17, CSF was obtained from the great cerebral cistern by puncture. Rats were anesthetized as described for stereotaxic injections and fixed to a 90° head angle in a stereotaxic device. A microsyringe carrying a 26G needle was fixed to the manipulator arm with both, the manipulator and the needle oriented vertically. The hair was removed from the dorsal surface of the skin, the zone between the parietal bone and

vertebral column was located by palpation and the middle point marked with a marker. The needle was introduced to a depth between 1.5–2.0 mm and the piston slowly pulled. This procedure allowed to obtain 50−80 μl CSF. Samples contaminated with blood were discarded.

Motor tests

On experimental days −3 (pre-treatment) and +16 (post-treatment) all rats were submitted to a battery of motor tests adapted in part from Wallace et al. (1980) and Biesiadecki et al. (1999).

Suspension from a horizontal wire mesh pole. The time during which the rats could sustain their own weight was determined by placing the animals on a horizontal wire mesh pole and immediately rotating the pole so that the animals were left suspended from the wire mesh 70 cm over a water tank. The latency for the animals to fall was recorded as the average of three consecutive tests.

Performance on a wire mesh ramp. A 90 cm long by 42 cm wide metal ramp set at an angle of 70° to the floor was used. The ramp was covered by a central strip of wire mesh (65×20 cm^2) to offer the animals a grip and the base of the ramp was submerged into water up to 15 cm to prevent the animals from descending to the floor. Animals were placed on the central strip and the latency for them to fall to the water was recorded as the average of three consecutive tests. If an animal lasted up to 120 s, it was removed from the ramp and its performance was recorded as maximal.

Performance on a rotating platform. Animals were placed on the centre of an elevated cylindrical plastic platform which was 30 cm in height and 8 cm in diameter. The motorized platform could perform an orbital rotational movement at different speeds (Decalab, FBR model, Buenos Aires, Argentina). In the present tests the animals were placed on the centre of the platform and the motor was immediately turned on and set at 30 rpm. The latency for the animals to fall off the platform was recorded as the average of two consecutive tests.

Brain and spinal cord processing and immunofluorescence

On experimental day +17 animals were placed under deep anesthesia and perfused with PBS and then with phosphate buffered para-formaldehyde 4%, (pH 7.4) fixative. The brain and spinal cord were rapidly removed and serially cut into 20 μm thick coronal sections using a vibratome (Leica VT 1000S, Germany). For vimentin immunofluorescence, spinal cord sections were incubated with a monoclonal mouse anti-vimentin antibody (DakoCytomation, Carpinteria, CA, USA), washed twice with PBS, incubated for 45 min with a 1:1000 Alexa555-conjugated goat anti-mouse IgG (Jackson Immuno Research) and counterstained for 15 min with the fluorescent DNA stain 4',6-diamidino-2-phenylindole (DAPI). Fluorescence was detected with an Olympus confocal microscope (Olympus FV1000) with an emission filter of 490–540 nm, for GFP detection (laser 473 nm); 575–675 nm for Alexa555 detection (laser 559 nm), 430−455 nm for DAPI detection (laser 405 nm) and 575–675 nm for Qdots detection (laser 405 nm). An objective of 40× (UPlanSAPO) with a NA of 0.95 was used.

Captured 16 bit monochrome TIFF pseudo-colored images were exported to an image analysis program (ImagePro Plus v 6.3, Media Cybernetics, USA) in order to perform the colocalisation analysis described below (Colocalisation analysis).

Colocalisation analysis

In RAd-$(TK/GFP)_{fus}$-injected young rats, colocalisation analysis, GFP and DAPI labeling was performed in images of the entire cervical spinal cord. Briefly, using the Color Composite function of the Process menu of the image analysis program, pseudo-colored images were taken in pairs of dyes. For quantifying the colocalisation indexes of both labels, the Colocalisation function of the software was used and the Mander overlap coefficient (R) calculated which is 0.0 for no colocalisation and 1.0 for 100% colocalisation of two intensity patterns (Agnati et al., 2005).

IGF-I assay

IGF-I was extracted from serum and CSF samples (20 μl) by acid-ethanol cryoprecipitation and was radioimmunoassayed as previously described (Hereñú et al., 2007) using antibody UB2-495 distributed by AF. Parlow, NHPP, NIDDK. Recombinant human IGF-I rhIGF-I (Cell Sciences Inc., Canton, MA, USA) was used as tracer and unlabeled ligand.

Statistical analysis

The one-sample two-tailed *t*-test for repeated measures was used for assessing motor data whereas the one way analysis of variance (ANOVA) was used to evaluate the IGF-I concentration data of Table 1. Bonferroni method was chosen as a post hoc test.

RESULTS

Expression of TK/GFP in the ependymal layer of cerebral ventricles

Injection of RAd$(TK/GFP)_{fus}$ in the LV induced expression of TK/GFP in the ependymal cell layer of all cerebral ventricles in both young (Fig. 2A–D) and aged (Fig. 3) rats as well as in the central canal at the level of the Obex (Fig. 2E). Fluorescence intensity was distributed evenly in the ependymal cell layer and was largely absent in the brain parenchyma. It remained at maximal levels in the transduced cells for up to 5 days post vector injection and as expected, TK/GFP expression became progressively weaker afterwards.

Low magnification sections revealed a predominant expression of TK/GFP in the ependymal cell layer of the rostral portion of the 4V, before the bifurcation of the lateral recesses (Fig. 2C) whereas fewer ependymal cells showed TK/GFP expression in the caudal portion, at the Obex of the medulla. Fluorescent cells were distributed evenly in the ependymal cell layer of the rostral 4V but were more scattered in the central canal at the Obex.

Table 1. Effect of i.c.v. RAd-IGF-I injection on IGF-I levels in CSF and serum of young and aged female rats

Experimental group	IGF-I in serum (ng/ml) Day 16 p.v.i.	IGF-I in CSF (ng/ml) Day 17 p.v.i.
Young-Rad-(TK/GFP) (5)*[a]	473±66	61±9
Young-RAd-IGF-I (5)	465±81	107±8
Aged-(Rad-TK/GFP) (4)[b]	344±69	25±6
Aged-RAd-IGF-I (4)	349±74	99±10

Data are expressed as 0±SEM.

* Numbers in parenthesis represent the number of animals assessed per group.

Significance of difference within age groups: [a] $P<0.01$; [b] $P<0.01$. Young vs. aged was $P<0.01$ for controls and NS for experimental animals.

p.v.i., post vector injection.

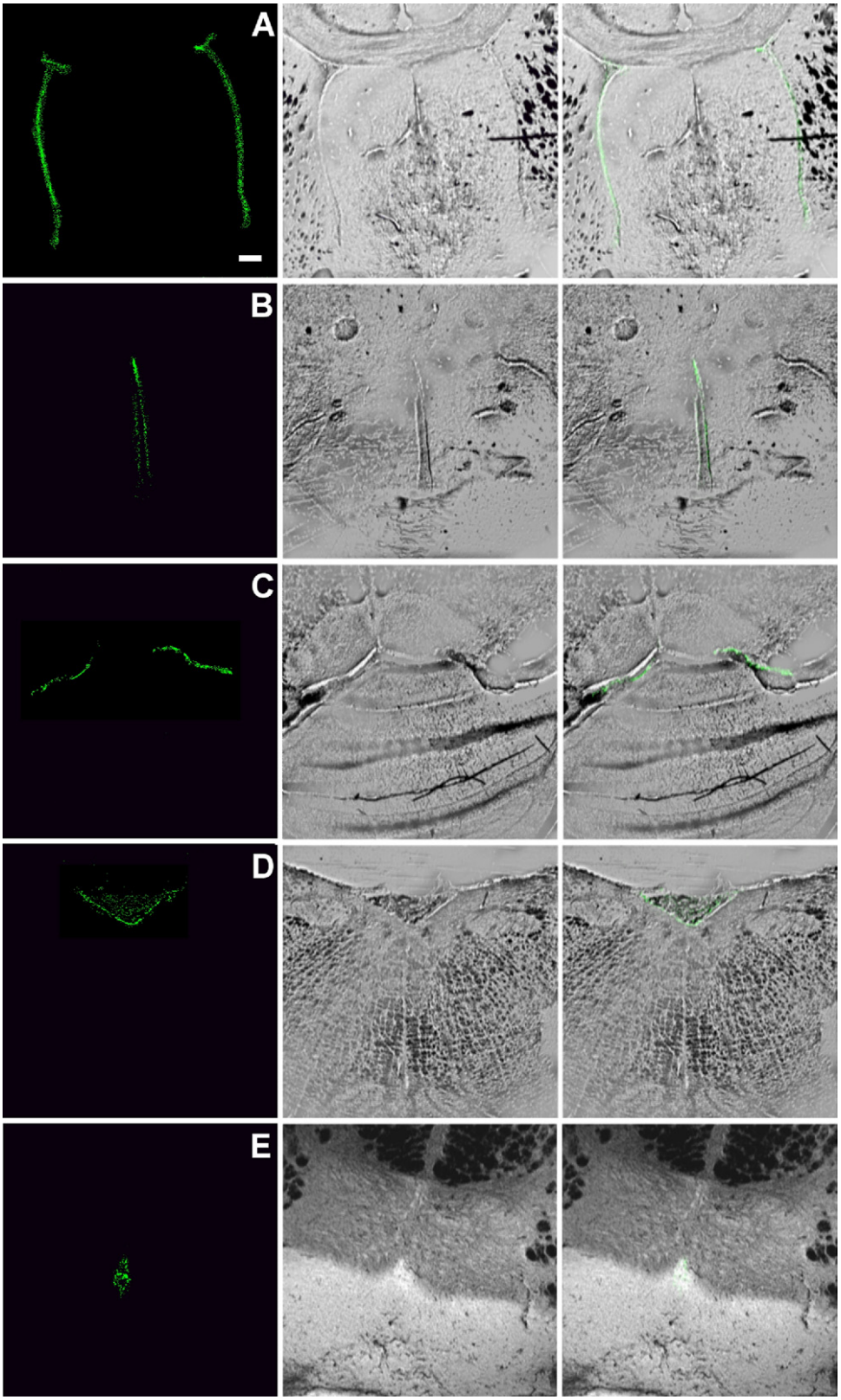

Fig. 2. TK/GFP expression at cerebral ventricles of young rats 3 d after RAd-$(TK/GFP)_{fus}$ injection in the LV. Confocal images of all cerebral ventricles are shown. Left panels show the expression of TK/GFP in the ependymal cell layer of cerebral ventricles. Centre panels show phase contrast of the corresponding left panels. Right panels represent a merge of the centre and left panels and show the anatomical location of fluorescent cells. (A) LV at 0.20 mm from bregma; (B) Third ventricle at −3.60 mm from bregma; (C) Lateral recesses of the 4V at −11.60 mm from bregma; (D) 4V at −13.24 mm from bregma; (E) Central canal at −13.68 mm from the bregma. Bar=250 μm. For interpretation of the references to color in this figure legend, the reader is referred to the Web version of this article.

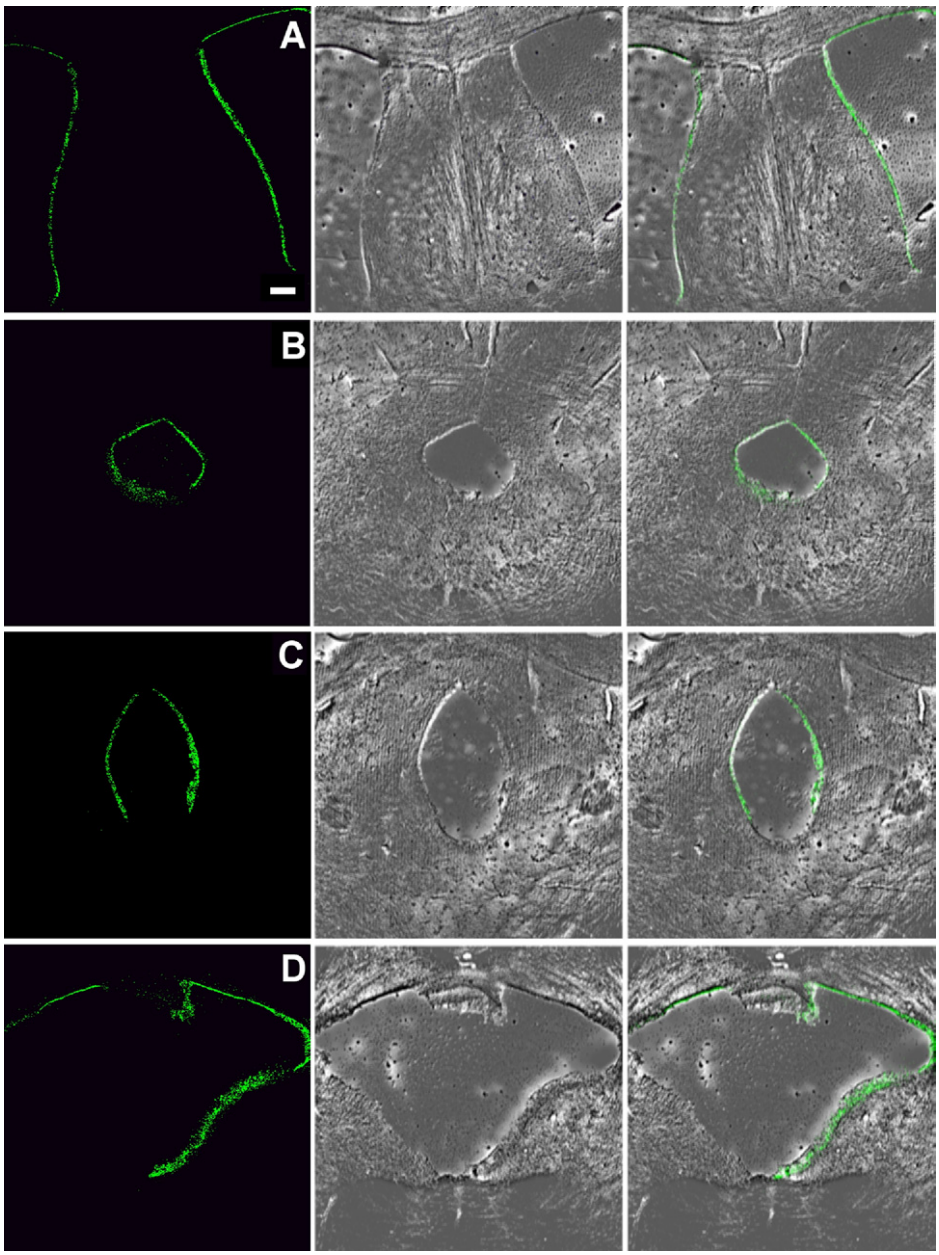

Fig. 3. TK/GFP expression at cerebral ventricles of aged rats 3 d after RAd-$(TK/GFP)_{fus}$ injection in the LV. Confocal images of the cerebral ventricles. Left panels show the expression of TK/GFP in all cerebral ventricles. Details are as in Fig. 2; (A) LV at −0.40 mm from bregma; (B) Sylvian aqueduct at −7.64 mm from bregma; (C) Recess of inferior colliculus at −8.72 mm from bregma; (D) 4V at −12.72 mm from bregma; Bar=250 μm. For interpretation of the references to color in this figure legend, the reader is referred to the Web version of this article.

Qualitatively, the density of fluorescent ependymocytes was comparable in the cerebral ventricles of young and aged rats (Figs. 2 and 3).

Expression of TK/GFP in the ependymal layer of the spinal cord

Expression of TK/GFP in the spinal cord was also restricted to the ependymal cell layer in both young (Fig. 4) and aged (Fig. 5) rats. It was only detected in the cervical portion of the spinal cord, irrespective of the site of vector injection (LV or 4V). In the young rats, the number of ependymocytes expressing the TK/GFP transgene decreased progressively from C1 to C6. No fluorescent cells were detected beyond C6. In the cervical spinal cord of aged rats the pattern of TK/GFP expression remained more or less constant throughout the six cervical segments. Again, no fluorescence was observed beyond C6.

When RAd$(TK/GFP)_{fus}$ was injected at the 4V, a slightly higher number of fluorescent cells was observed in the first three cervical segments but again, fluorescence was not observed beyond C6. Rostral to the injection site we observed TK/GFP expression in the

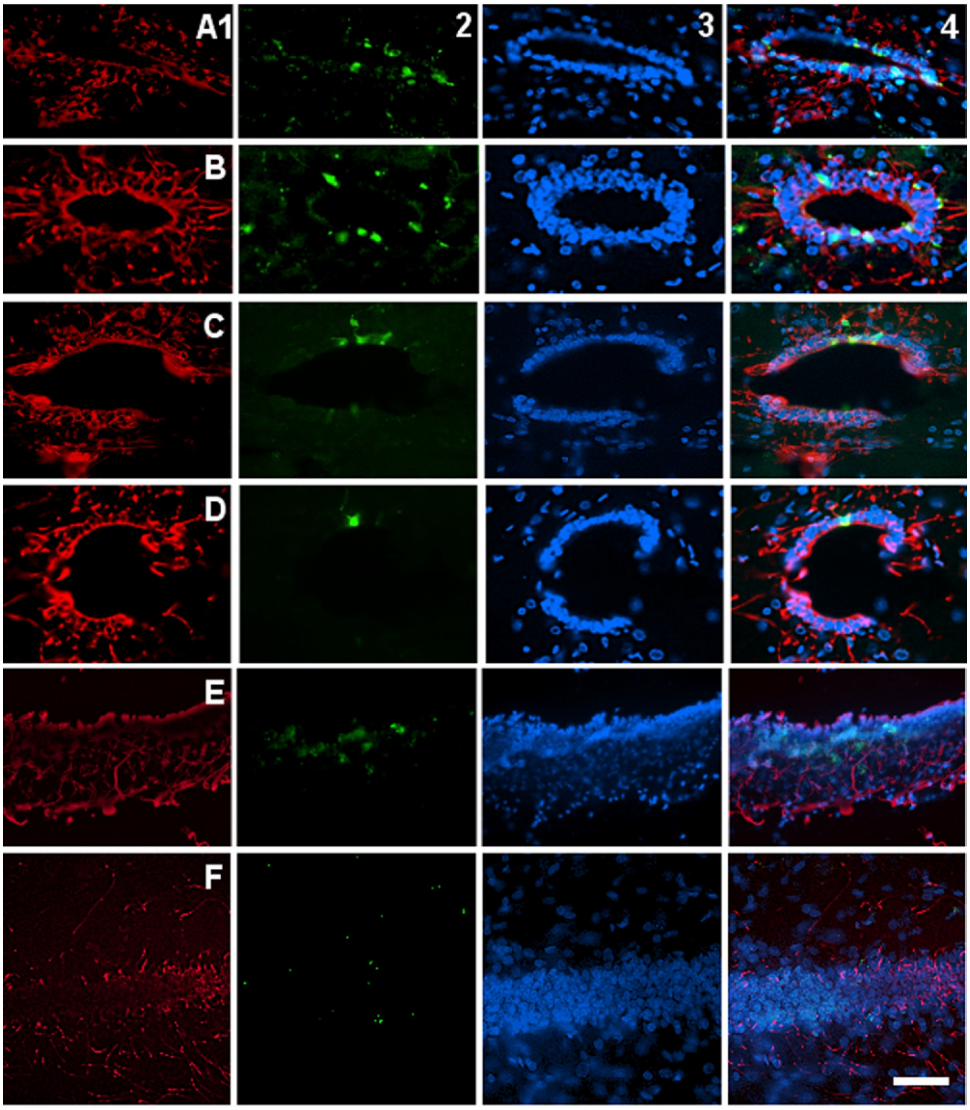

Fig. 4. Expression of TK/GFP in the ependymal cell layer of the spinal cord of young rats 3 d after RAd-$(TK/GFP)_{fus}$ injection in the LV. 20-μm thick slices of spinal cord segments were incubated with anti-vimentin using Alexa555-conjugated goat anti-mouse IgG as secondary antibody. Slices were counterstained with DAPI. Column 1 shows vimentin staining of the ependymal cells in the cervical segments. Column 2 represents the expression of TK/GFP in the ependymal cells of different cervical segments. Column 3 shows the staining of nuclei with DAPI. Column 4 represents the merging of the other three columns. Rows (A–D) are coronal sections of the following segments: (A) C1; (B) C3; (C) C5 and (D) C6. Rows (E) and (F) are longitudinal sections at the ependymal level of the following segments: (E) C2 and (F) C4. Bar for all the segments=100 μm. For interpretation of the references to color in this figure legend, the reader is referred to the Web version of this article.

lateral recesses but not in the rostral portion of the 4V (data not shown).

In the young rats, co-incubation of cervical spinal cord sections with the DNA dye DAPI and an anti-vimentin antibody (vimentin is an intermediate filament present in the cytoplasm of ependymocytes), confirmed the high affinity of the vector for ependymal cells as only few vimentin-negative cells expressed TK/GFP (Fig. 4). Quantitative colocalisation analysis (R overlap coefficient×100; 0±SEM) performed on five sections corresponding to every cervical segment with a separation of 100 μm between them, indicated a 94.7±1.3% colocalisation for TK/GFP fluorescence with DAPI (cyan expression). For the aged rats (Fig. 5), colocalisation of TK/GFP expression and DAPI showed an R overlap coefficient of 91.2±1.7%.

Continuity of the 4V with the central spinal canal

In order to determine whether there is a physical continuity of the 4V with the spinal canal which would have allowed our viral vectors to directly reach the spinal ependymocytes, serial coronal sections from the Obex to the cervical spinal canal were assessed. The anatomical evidence showed an apparent physical continuity between the 4V and the spinal canal (Fig. 6). This continuity was confirmed by independent experiments using fluorescent nanoparticles. Ten minutes after injection of Qdots

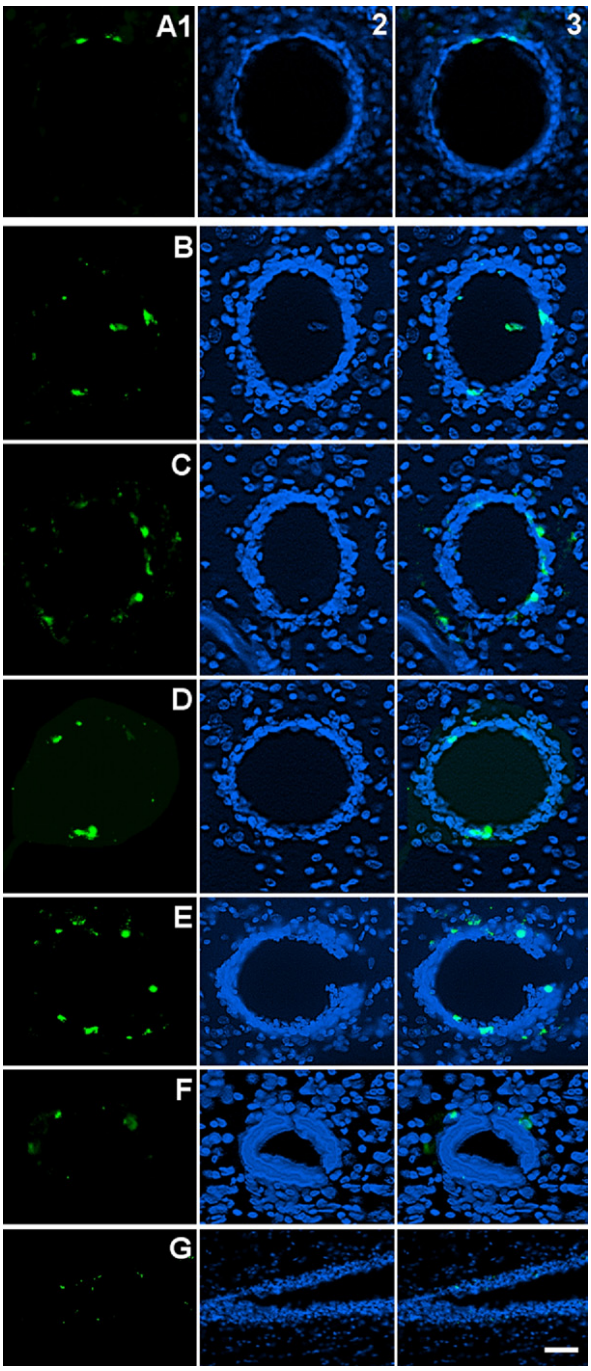

Fig. 5. Expression of TK/GFP in the ependymal cell layer of the spinal cord of aged rats 3 d after RAd-$(TK/GFP)_{fus}$ injection in the LV. 20-μm thick slices of spinal cord segments were counterstained with DAPI. Column 1 represents the expression of TK/GFP in the ependymal cells of different cervical segments. Column 2 shows the staining of nuclei with DAPI. Column 3 represents the merging of the previous columns. Rows (A–F) are coronal sections of the following segments: (A) C1; (B) C2; (C) C3; (D) C4; (E) C5 and (F) C6. Row (G) is the longitudinal section at the ependymal level of C4. Bar for (A–F)=50 μm; for (G)=200 μm. For interpretation of the references to color in this figure legend, the reader is referred to the Web version of this article.

at the 4V, the ependyma of the upper cervical segments showed moderate fluorescence whereas the C6 segments showed the highest level of ependymal fluorescence. Beyond C6 less intense fluorescence was detectable (Fig. 7).

Restorative effects of IGF-I gene therapy on motor performance in aging rats

A significant age-related reduction in CSF levels of IGF-I occurred in the control rats. i.c.v. injection of RAd-IGF-I, but not $RAd(TK/GFP)_{fus}$, induced a significant increase in IGF-I levels in the CSF, 17 days post-vector injection (Table 1). The data shown in Table 1 represent IGF-I levels in the CSF sampled from the cisterna magna and these levels may not be necessarily the same in the CSF at distal regions of the cerebral ventricles or central canal of spinal cord. Furthermore, since our RIA measured total IGF-I, the fraction of IGF-I bound to IGF-I binding proteins is not known. Serum analysis for IGF-I did not show significant differences among groups before and after vector injection (Table 1).

Motor tests were conducted in young and aged rats except for the "Performance on a rotating platform (see *Performance on a rotating platform.* under Motor tests)" test which was only done in the aged animals due to the fact that young rats jumped off the platform at the very beginning of the test irrespective of the treatment. When the other two tests ("Suspension from a horizontal wire mesh pole" and "Performance on a wire mesh ramp", see *Suspension from a horizontal wire mesh pole.* and *Performance on a wire mesh ramp.*, respectively under Motor tests) were performed before vector injection, they confirmed a marked age-related decline in motor performance (Fig. 8, main panels). The same two tests performed 16 days after RAd-IGF-I or $RAd(TK/GFP)_{fus}$ (control) i.c.v administration showed that IGF-I gene therapy had no effect on motor performance in young rats (Fig. 8, insets). In fact, motor performance fell slightly in the young animals after vector injection in both experimental and control animals (Fig. 8, insets). In the aged animals 16-day IGF-I gene therapy induced a significant improvement in the performance of the animals in the "Performance on a wire mesh ramp" and "Performance on a rotating platform" tests. In the highly demanding "Suspension from a horizontal wire mesh pole" tests IGF-I gene therapy did not have a significant effect (Fig. 8, insets).

DISCUSSION

The present results show that RAd-IGF-I but not $RAd(TK/GFP)_{fus}$ gene therapy delivered by the i.c.v. route induce a moderate but significant improvement in motor activity of aged rats, without affecting performance of young animals.

Our results also demonstrate that the high affinity of adenoviral vectors for ependymocytes can be exploited to implement IGF-I gene therapy in the spinal cord without performing direct vector injections in the spinal cord or brain parenchyma. Previous studies indicate that there appears to be substantial therapeutic benefit to increasing CSF levels of IGF-I in different animal models of brain aging or injury. For example, i.c.v. administration of IGF-I

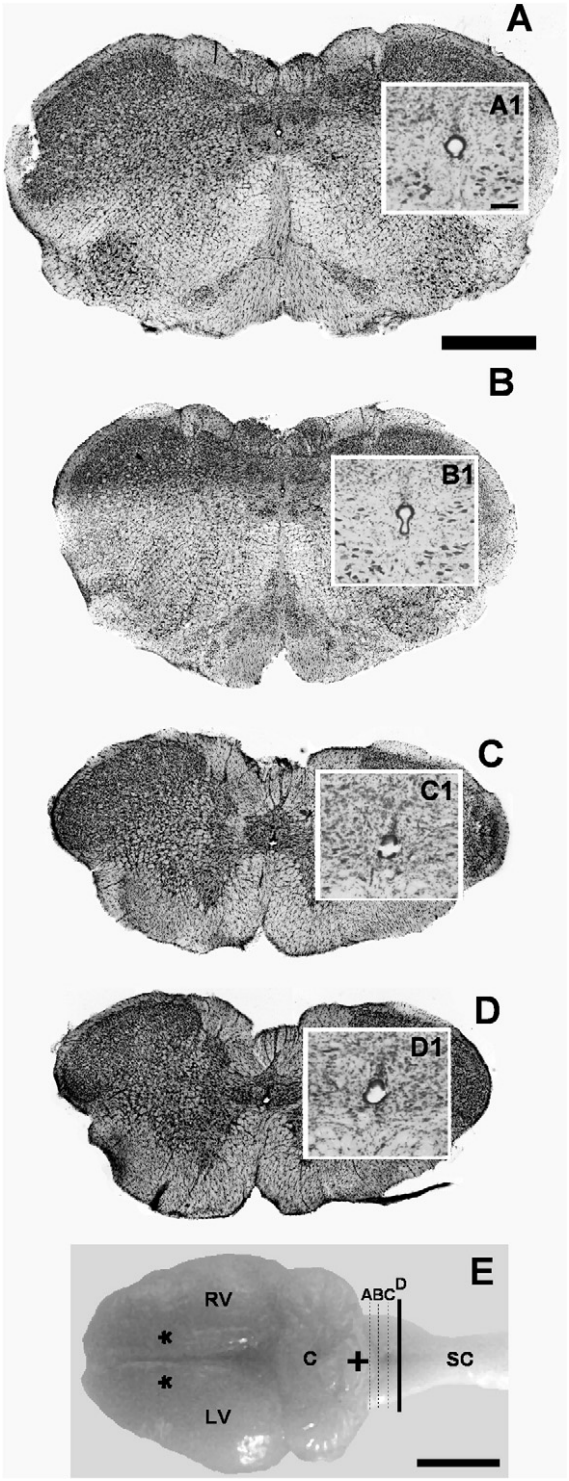

Fig. 6. Anatomical continuity of the central canal from medulla through spinal cord. (A) Coronal section at −14.08 mm from bregma; (B) Coronal section at −14.30 mm from bregma; (C) Coronal section at −14.60 mm from bregma. Insets (A1–C1) show the central canal in the caudal portion of the 4V. (D) Coronal section at rostral portion of the spinal cord C1 segment. Notice the emergence of the first cervical ventral root which provides a precise indication of the boundary between the medulla and the cervical spinal cord. Inset (D1) shows the central canal at C1. Bars for (A–D)=1 mm. Bars for Insets (A1–D1)=200 μm. Cresyl Violet stain. (E) Photography of a young female rat CNS showing left and right hemispheres (LH and RH, respectively), cerebellum (C) and spinal cord (SC). Asterisks show the injection site of the viral vector (bregma −0.8 mm anteroposterior, 3.7 mm dorsoventral and ±1.5 mm mediolateral). The cross indicates the injection site into the 4V caudal to the lateral recesses used in some rats (bregma, −13.3 mm anteroposterior, 7.5 mm dorsoventral, and 0 mm mediolateral, at the midline). The solid black line crossing the nervous structure indicates the transition limit between the medulla and the C1 segment of the spinal cord. Dotted lines indicate where sections (A–C) described above were obtained from. Bar=0.5 cm.

to 29 months old rats using osmotic minipumps ameliorated the age-related decline in hippocampal neurogenesis (Lichtenwalner et al., 2001), increased the rates of local cerebral glucose utilization (Lynch et al., 2001), and hippocampal NMDAR2A and R2B subunit expression (Sonntag et al., 2000). Furthermore, 28-day i.c.v. infusion of IGF-I, using osmotic minipumps, attenuated age-related deficits in working and reference memory assessed in the Morris water maze and object recognition tasks (Markowska et al., 1998). The present results show that increasing IGF-I in the CSF can also have a restorative effect on motor performance in aging rats. Our finding that the motor performance of young rats was not enhanced by IGF-I gene therapy is in line with previous studies in the hypothalamus of aging rats in which it was reported that intrahypothalamic IGF-I gene therapy restored dopaminergic neuron function in aging rats but did not induce any change in young animals (Hereñú et al., 2007). A possible explanation for these observations may be that IGF-I is a neurorestorative molecule but it does not increase the function of healthy neurons. Since our results reveal a significant fall of IGF-I levels in the CSF of the aged animals, the correction of this deficit by IGF-I gene therapy may have contributed to restore motor performance in the old rats. Since our adenovector showed extensive transduction in the cervical spinal cord but not below, we focused our motor tests on forelimbs performance.

IGF-I receptors and binding proteins are expressed in many regions of the CNS, including the spinal cord ventral gray matter (Bondy and Cheng, 2004). This peptide is a prototypical neuronal survival factor that exerts prosurvival effects specifically on motor neurons (Doré et al., 1997). Early clinical trials (Lai et al., 1997; Borasio et al., 1998) showed little benefit, if any, of systemically administered recombinant IGF-I in amyotrophic lateral sclerosis (ALS) patients. This may have been due to lack of sustained delivery, sequestration of exogenous IGF-I by high levels of systemic and/or CNS IGF-I binding proteins, and low efficiency of protein delivery to motor neurons via systemic injections. In this context, viral vector delivery appears as an attractive alternative strategy for achieving sustained long-term expression of neurotrophic factors like IGF-I in the spinal cord, while avoiding unwanted side effects and peripheral IGF-I sequestration. Recently, direct intraparenchymal lumbar spinal cord injection of an adeno-associated vector type 2 (AAV2) expressing IGF-I to transgenic $SOD1^{G93A}$ mice, a model of ALS, resulted in robust spinal cord IGF-I expression in the injection region as well as a partial rescue of lumbar spinal cord motor neurons. In

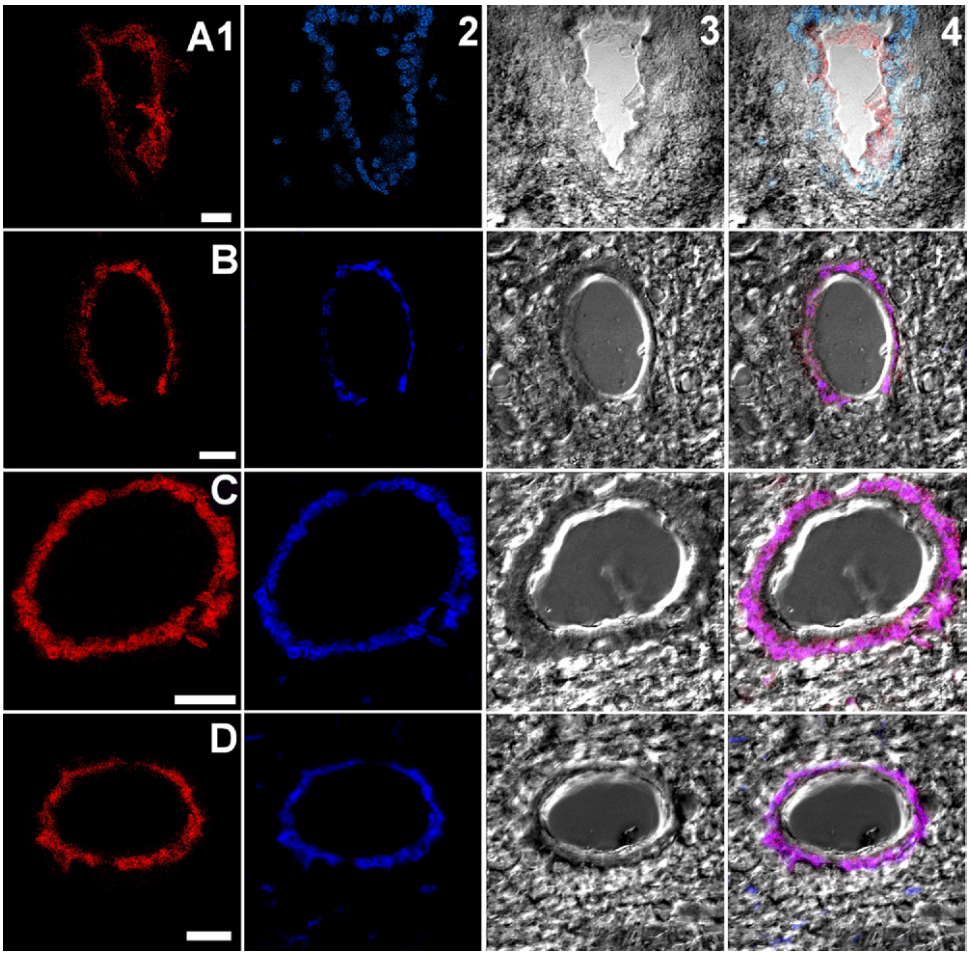

Fig. 7. Anatomical continuity of the central canal from medulla through spinal cord detected using Qdots. Ten μl Qdots in PBS were injected in the 4V of young rats and animals sacrificed 10 min afterwards. (A) Central canal of the medulla; (B) central canal at C2; (C) central canal at C6; (D) central canal at C8. Column 1 Qdots; Column 2 DAPI; Column 3 phase contrast of the corresponding previous panels; Column 4 represents a merge of the first three columns and shows the anatomical location of fluorescence. Bar=20 μm. For interpretation of the references to color in this figure legend, the reader is referred to the Web version of this article.

males, there was a delayed disease onset, delayed body weight loss and also a delayed decline in hindlimb grip strength as well as an increased animal survival (Lepore et al., 2007). In ALS rats (transgenic for SOD^{G93A}), cervical intraspinal delivery of an AAV expressing IGF-I resulted in reduced cervical motor neuron loss and preservation of motor function (forelimb grip strength) in males but not females (Franz et al., 2009). Although these studies revealed that direct viral vector-mediated IGF-I gene therapy is a promising therapeutic strategy in the spinal cord, intraspinal injection of vectors is a significantly invasive approach. The present study shows that the ependymal route, which is a much less invasive approach, is an effective alternative route for IGF-I delivery to the spinal cord. One important advantage of this method is that recombinant IGF-I is delivered to the CSF, the physiologic milieu from which liver-derived IGF-I is transported to target regions of the CNS. Furthermore the i.c.v. route allows recombinant IGF-I to reach the whole spinal cord, which in general will be a benefit for the treatment of ALS and other spinal cord pathologies. Although in rodents it is not feasible to inject a viral vector by lumbar puncture, the procedure would be possible in human patients thus substantially reducing the invasiveness of the procedure.

Our results suggest a physical continuity between the 4V and central spinal canal. We did not find reports documenting such physical continuity. CSF is produced in the choroid plexuses of the LV, third and 4V. It is present in all of the ventricles, central canal of spinal cord and subarachnoid space of the brain and spinal cord (Segal, 2005). According to the literature the flow pattern of the CSF begins in the choroid plexuses and flows downstream from rostral to caudal part of the CNS. In the 4V it flows out into the subarachnoid space via the lateral recesses, foramina of Luschka and Magendie (Segal, 2005; Cerda-Gonzalez et al., 2009; Stadlbauer et al., 2010). According to Stoodley et al. (1996) CSF present in the central canal comes from the subarachnoid spaces flowing into the perivascular spaces and across the interstitial space reaches the central canal. Moreover, according to Cifuentes et al. (1992) CSF flowing from the subarachnoid space is directed towards type-B vessels (those intruding into the spinal cord

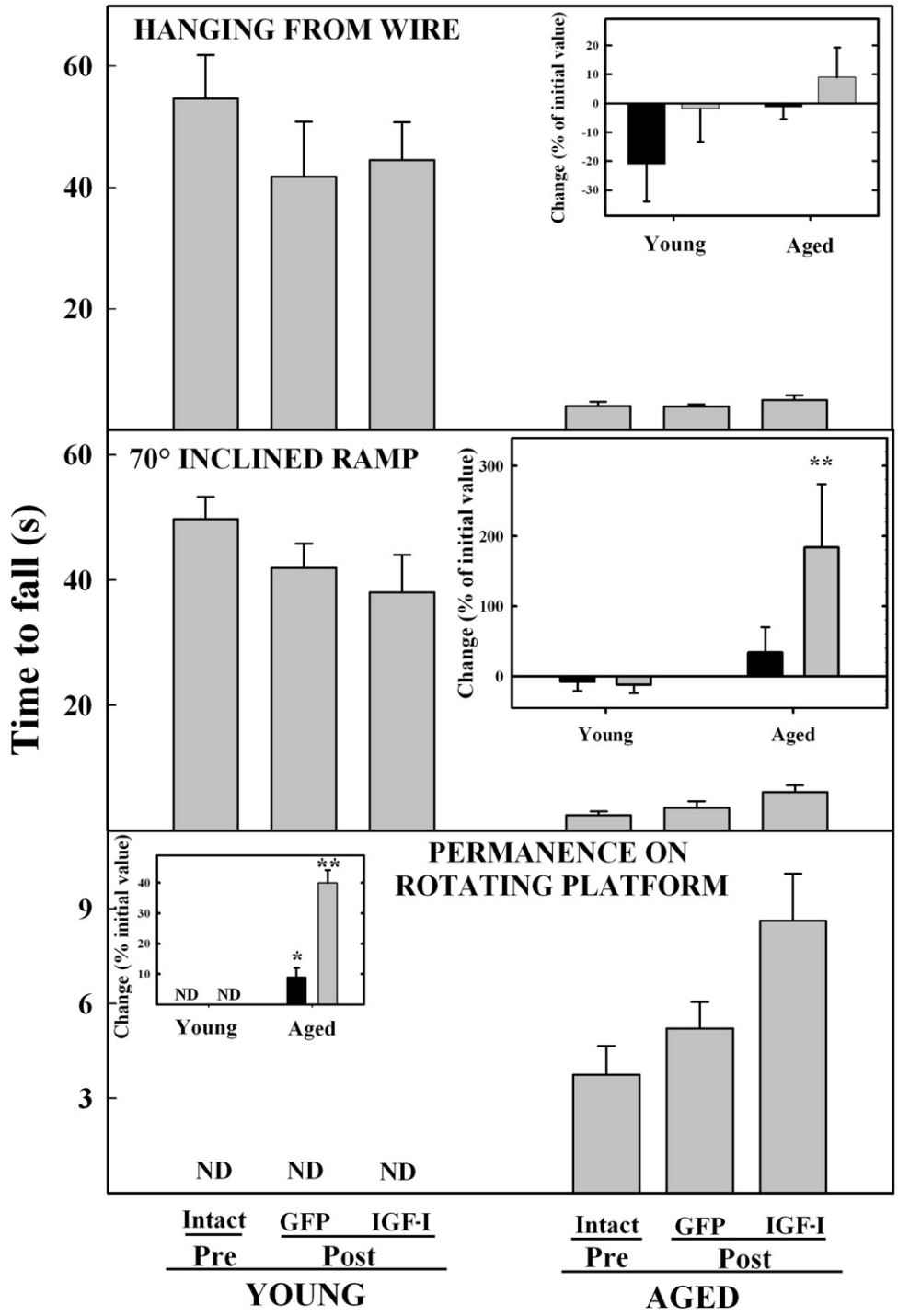

Fig. 8. Restorative effect of i.c.v. IGF-I gene therapy on motor performance in aged rats. The upper panel shows the resistance of rats to fall from a horizontal pole from which they hang. The middle panel shows the ability of rats to remain on a ramp set at 70° to the horizontal. The lower panel shows the endurance of rats on top of a rotating platform. Main panels represent absolute values (in s) whereas insets represent percentage of change from corresponding vector preinjection values. [% change=(post injection value−pre injection value)×100/pre injection value]. The motor performance of the animals fell after stereotaxic surgery, particularly in the young rats, whose initial motor performance had been substantially higher than that of the aged rats. Solid columns in the insets correspond to RAd-$(TK/GFP)_{fus}$-injected rats while light gray columns correspond to RAd-IGF-injected animals. Error bars represent SEM (n=6 animals per group). ND, not determined. Young: 5 mon; aged: 30 mon. In the insets asterisks over bars represent significance of difference of column value from zero. * $P<0.05$; ** $P<0.01$.

from the medial ventral sulcus and occupying the anterior commissure of the gray matter) thus spreading into the labyrinths, the intercellular space of the ependymal lining, and the lumen of the central canal. In our study we have

found viral expression in the ependymal cell layer of the first six spinal cord segments. The results from the Qdots experiments strengthen the idea that physical nanoparticles (viral or inorganic) have similar diffusional pattern within the central canal, reaching the cervical segments. Despite the apparently limited diffusion of viral vectors down the spinal canal it seems reasonable to assume that transgenic IGF-I levels in the CSF are also high in the CSF flowing in the thoracic and lumbar segments of the spinal cord, coming from both the spinal cord central canal and the subarachnoid space. As mentioned above, serum IGF-I is known to be actively transported through the choroid plexuses and translocated to the CSF from where the molecule reaches specific areas of the brain and possibly the spinal cord, by yet unidentified mechanisms (Guan et al., 1996; Carro et al., 2006). Since we used the gene for rat IGF-I and endogenous IGF-I is present in the CNS, the distribution of transgenic IGF-I could not be determined in the brain or spinal cord parenchyma. Nevertheless, it seems reasonable to assume that transgenic IGF-I reached the same physiologic targets than the endogenous peptide present in the CSF. Whether the restorative effects observed in the aged rats was the result of additive effects of transgenic IGF-I acting at multiple CNS regions or a restorative action on a single (or few) critical CNS areas, remains to be clarified.

CONCLUSIONS

We conclude that i.c.v. IGF-I gene therapy partially, but significantly, restores motor coordination and forelimb grip strength in aged females and that the ependymal route emerges as a promising approach for implementing minimally invasive IGF-I gene therapy in the aging brain and spinal cord.

Acknowledgments—This work was partially financed by grant PICT 2006-583 from the National Agency for Promotion of Science and Technology (ANPCyT) to ELP, and NIH grant R01AG029798-3 from the National Institute on Aging (NIA) and the Fogarty International Center (FIC) to RGG. CBH, RGG and ELP are Research Career scientists of the Argentine Research Council (CONICET). GRM holds a post doc fellowship from CONICET. We gratefully thank Dr. A. Delorenzi for his critical reading of the manuscript and relevant comments.

REFERENCES

Agnati LF, Fuxe K, Torvinen M, Genedani S, Franco R, Watson S, Nussdorfer GG, Leo G, Guidolin D (2005) New methods to evaluate colocalization of fluorophores in immunocytochemical preparations as exemplified by a study on A2A and D2 receptors in Chinese hamster ovary cells. J Histochem Cytochem 53:941–953.

Beilharz EJ, Russo VC, Butler G, Baker NL, Connor B, Sirimanne ES, Dragunow M, Werther GA, Gluckman PD, Williams CE, Scheepens A (1998) Co-ordinated and cellular specific induction of the components of the IGF/IGFBP axis in the rat brain following hypoxic–ischemic injury. Brain Res Mol Brain Res 59:119–134.

Biesiadecki BJ, Brand PH, Koch LG, Metting PJ, Britton SL (1999) Phenotypic variation in sensorimotor performance among eleven inbred rat strains. Am J Physiol Regul Integr Comp Physiol 276: 1383–1389.

Bilak MM, Corse AM, Kuncl RW (2001) Additivity and potentiation of IGF-I and GDNF in the complete rescue of postnatal motor neurons. Amyotroph Lateral Scler Other Motor Neuron Disord 2: 83–91.

Bondy CA, Cheng CM (2004) Signaling by insulin-like growth factor 1 in brain. Eur J Pharmacol 490:25–31.

Borasio GD, Robberecht W, Leigh PN, Emile J, Guiloff RJ, Jerusalem F, Silani V, Vos PE, Wokke JH, Dobbins T (1998) A placebo-controlled trial of insulin-like growth factor-I in amyotrophic lateral sclerosis. European ALS/IGF-I Study Group. Neurology 51: 583–586.

Burek JD (1978) Pathology of aging rats. Boca Ratón: CRC Press.

Carro E, Nuñez A, Busiguina S, Torres-Aleman I (2000) Circulating insulin-like growth factor I mediates effects of exercise on the brain. J Neurosci 20:2926–2933.

Carro E, Trejo JL, Spuch C, Bohl D, Heard JM, Torres-Aleman I (2006) Blockade of the insulin-like growth factor I receptor in the choroid plexus originates Alzheimer's-like neuropathology in rodents: new cues into the human disease? Neurobiol Aging 27:1618–1631.

Cerda-Gonzalez S, Olby NJ, Broadstone R, McCullough S, Osborne JA (2009) Characteristics of cerebrospinal fluid flow in Cavalier King Charles Spaniels analyzed using phase velocity cine magnetic resonance imaging. Vet Radiol Ultrasound 50:467–476.

Cifuentes M, Fernandez LL, Perez J, Perez Figares JM, Rodriguez EM (1992) Distribution of intraventricularly injected horseradish peroxidase in cerebrospinal fluid compartments of the rat spinal cord. Cell Tissue Res 270:485–494.

Daughaday WH, Rotwein P (1989) Insulin-like growth factors I and II: peptide, messenger ribonucleic acid and gene structures, serum, and tissue concentrations. Endocr Rev 10:68–91.

Doré S, Kar S, Quirion R (1997) Rediscovering an old friend, IGF-I: potential use in the treatment of neurodegenerative diseases. Trends Neurosci 20:326–331.

Fontana PA, Barbeito CG, Goya RG, Gimeno EJ, Portiansky EL (2009) Impact of very old age on the expression of cervical spinal cord cell markers in rats. J Chem Neuroanat 37:98–104.

Franz CK, Federici T, Yang J, Backus C, Oh SS, Teng Q, Carlton E, Bishop KM, Gasmi M, Bartus RT, Feldman EL, Boulis NM (2009) Intraspinal cord delivery of IGF-I mediated by adeno-associated virus 2 is neuroprotective in a rat model of familial ALS. Neurobiol Dis 33:473–481.

García-Segura LM, Diz-Chaves Y, Perez-Martín M, Darnaudéry M (2007) Estradiol, insulin-like growth factor-I and brain aging. Psychoneuroendocrinology 32 (Suppl 1):S57–S61.

Guan J, Skinner SJ, Beilharz EJ, Hua KM, Hodgkinson S, Gluckman PD, Williams CD (1996) The movement of IGF-1 into the brain parenchyma after hypoxic–ischaemic injury. Neuroreport 7:632–636.

Hereñú CB, Cristina C, Rimoldi OJ, Becú-Villalobos D, Cambiaggi V, Portiansky EL, Goya RG (2007) Restorative effect of Insulin-like Growth Factor-I gene therapy in the hypothalamus of senile rats with dopaminergic dysfunction. Gene Ther 14:237–245.

Hereñú CB, Sonntag WE, Morel GR, Portiansky EL, Goya RG (2009) The ependymal route for Insulin-like Growth Factor-I gene therapy in the brain. Neuroscience 163:442–447.

Hitt M, Bett A, Prevec L, Graham FL (1998) Construction and propagation of human adenovirus vectors. In: Cell biology: a laboratory handbook (Hitt M, Bett A, Prevec L, Graham FL, eds), pp 1500–1512. San Diego: Academic Press.

Kane CJ, Sims TJ, Gilmore SA (1997) Astrocytes in the aged rat spinal cord fail to increase GFAP mRNA following sciatic nerve axotomy. Brain Res 759:163–165.

Lai EC, Felice KJ, Festoff BW, Gawel MJ, Gelinas DF, Kratz R, Murphy MF, Natter HM, Norris FH, Rudnicki SA (1997) Effect of recombinant human insulin-like growth factor-I on progression of ALS. A placebo-controlled study. The North America ALS/IGF-I Study Group. Neurology 49:1621–1630.

Lepore AC, Haenggeli C, Gasmi M, Bishop KM, Bartus RT, Maragakis NJ, Rothstein JD (2007) Intraparenchymal spinal cord delivery of adeno-associated virus IGF-1 is protective in the SOD1G93A model of ALS. Brain Res 1185:256–265.

Li XS, Williams M, Bartlett WP (1998) Induction of IGF-1 mRNA expression following traumatic injury to the postnatal brain. Brain Res Mol Brain Res 57:92–96.

Lichtenwalner RJ, Forbes ME, Bennett SA, Lynch CD, Sonntag WE, Riddle DR (2001) Intracerebroventricular infusion of insulin-like growth factor-I ameliorates the age-related decline in hippocampal neurogenesis. Neuroscience 107:603–613.

Lynch CD, Lyons D, Khan A, Bennett SA, Sonntag WE (2001) Insulin-like growth factor-1 selectively increases glucose utilization in brains of aged animals. Endocrinology 142:506–509.

Markowska AL, Mooney M, Sonntag WE (1998) Insulin-like growth factor-1 ameliorates age-related behavioral deficits. Neuroscience 87:559–569.

Paquin A, Jaalouk DE, Galipeau J (2001) Retrovector encoding a green fluorescent protein–herpes simplex virus thymidine kinase fusion protein serves as a versatile suicide/reporter for cell and gene therapy applications. Hum Gene Ther 12:13–23.

Paxinos G, Watson C (1998) The rat brain in stereotaxic coordinates. San Diego: Academic Press.

Payne AM, Messi ML, Zheng Z, Delbono O (2007) Motor neuron targeting of IGF-1 attenuates age-related external Ca2+-dependent skeletal muscle contraction in senescent mice. Exp Gerontol 42:309–319.

Portiansky EL, Barbeito CG, Gimeno EJ, Zuccolilli GO, Goya RG (2006) Loss of NeuN immunoreactivity in rat spinal cord neurons during aging. Exp Neurol 202:519–521.

Rodrigues de Amorim MA, García-Segura LM, Goya RG, Portiansky EL (2010) Decrease in PTEN and increase in Akt expression and neuron size in aged rat spinal cord. Exp Gerontol 45:457–463.

Sanchez HL, Silva LB, Portiansky EL, Hereñú CB, Goya RG, Zuccolilli GO (2008) Dopaminergic mesencephalic systems and motor performance in very old rats. Neuroscience 154:1598–1606.

Segal MB (2005) Fluid compartments of the central nervous system. In: The blood-cerebrospinal fluid barrier, chapter 4 (Zheng W, Chodobski A, eds), pp 83–100. Boca Ratón: Chapman & Hall/CRC.

Sonntag WE, Bennett SA, Khan AS, Thornton PL, Xu X, Ingram RL, Brunso-Bechtold JK (2000) Age and insulin-like growth factor-1 modulate N-methyl-D-aspartate receptor subtype expression in rats. Brain Res Bull 51:331–338.

Sonntag WE, Ramsey M, Carter CS (2005) Growth hormone and insulin-like growth factor-1 (IGF-1) and their influence on cognitive aging. Ageing Res Rev 4:195–212.

Stadlbauer A, Salomonowitz E, van der Riet W, Buchfelder M, Ganslandt O (2010) Insight into the patterns of cerebrospinal fluid flow in the human ventricular system using MR velocity mapping. Neuroimage 51:42–52.

Stoodley MA, Jones NR, Brown CJ (1996) Evidence for rapid fluid flow from the subarachnoid space into the spinal cord central canal in the rat. Brain Res 707:155–164.

Wallace JE, Krauter EE, Campbell BA (1980) Motor and reflexive behavior in the aging rat. J Gerontol 35:364–370.

Walter HJ, Berry M, Hill DJ, Logan A (1997) Spatial and temporal changes in the Insulin-like growth factor (IGF) axis indicate autocrine/paracrine actions of IGF-I within wounds of the rat brain. Endocrinology 138:3024–3034.

Yao DL, West NR, Bondy CA, Brenner M, Hudson LD, Zhou J, Collins GH, Webster HD (1995) Cryogenic spinal cord injury induces astrocytic gene expression of insulin-like growth factor I and insulin-like growth factor binding protein 2 during myelin regeneration. J Neurosci Res 40:647–659.

(Accepted 6 January 2011)
(Available online 14 January 2011)